

MOL #35550

Title Page

Functional characterization of the promoter of human carbonyl reductase 1 (*CBR1*). Role of *XRE* elements in mediating induction of *CBR1* by ligands of the aryl hydrocarbon receptor

Sukhwinder S. Lakhman, Xiaomin Chen, Vanessa Gonzalez-Covarrubias,

Erin G. Schuetz, and Javier G. Blanco

Department of Pharmaceutical Sciences, The State University of New York at Buffalo,
Buffalo, NY (S.S.L, X.C, V. G-C, and J.G.B)

Department of Pharmaceutical Sciences, St. Jude Children Research Hospital,
Memphis, TN (E.G.S)

MOL #35550

Running Title Page

a) Running Title

Characterization of the Promoter of Human Carbonyl Reductase 1 (*CBR1*)

b) Corresponding author

Javier G. Blanco, PhD
545 Cooke Hall
Department of Pharmaceutical Sciences
The State University of New York at Buffalo
Buffalo, NY 14260-1200
Telephone: 716-645-2854 ext. 545
Fax: 716-645-3693
Email: jgblanco@buffalo.edu

c) Number of text pages: 24

Number of tables: 0

Number of figures: 9

Number of references: 34

Number of words in the Abstract: 227

Number of words in the Introduction: 638

Number of words in the Discussion: 868

d) List of nonstandard abbreviations

XRE, xenobiotic response element; TCDD, 2,3,7,8-tetrachlorodibenzo-p-dioxin;
TCPOBOP, 1,4-bis-[2-(3,5-dichloropyridyloxy)]-benzene

MOL #35550

ABSTRACT

Human carbonyl reductase 1 (*CBR1*) metabolizes a variety of substrates including the anticancer doxorubicin and the antipsychotic haloperidol. The transcriptional regulation of *CBR1* has been largely unexplored. Therefore, we first investigated the promoter activities of progressive gene-reporter constructs encompassing up to 2.4 kb upstream the translation start site of *CBR1*. Next, we investigated whether *CBR1* mRNA levels were altered in cells incubated with prototypical receptor activators (e.g. dexamethasone and rifampicin). *CBR1* mRNA levels were significantly induced (5-fold) by the ligand of the aryl hydrocarbon receptor (AHR) β-naphthoflavone. DNA sequence analysis revealed two xenobiotic response elements (-₁₂₂XRE, and -₅₇₈₃XRE) with potential regulatory functions. *CBR1* promoter constructs lacking the -₁₂₂XRE showed diminished (9-fold) promoter activity in AHR proficient cells incubated with β-naphthoflavone. Fusion of -₅₇₈₃XRE to the -₂₄₈₅*CBR1* reporter construct enhanced its promoter activity after incubations with β-naphthoflavone by 5-fold. Furthermore, we tested whether the potent AHR ligand 2,3,7,8-tetrachlorodibenzo-p-dioxin (TCDD) induced *Cbr1* expression in *Ahr*^{+/−} and *Ahr*^{−/−} mice. TCDD induced hepatic *Cbr1* mRNA (TCDD: 2-fold) and *Cbr1* protein levels (TCDD: 2-fold) in *Ahr*^{+/−} mice as compared to vehicle-injected controls. In contrast, no significant *Cbr1* mRNA and *Cbr1* protein induction was detected in livers from *Ahr*^{−/−} mice treated with TCDD. These studies provide the first insights on the functional characteristics of the human *CBR1* gene promoter. Our data indicate that the AHR pathway contributes to the transcriptional regulation of *CBR1*.

MOL #35550

INTRODUCTION

Human carbonyl reductase 1 (CBR1) catalyzes the NADPH-dependent reduction of a variety of xenobiotic compounds including smoke derived carcinogens and many relevant pharmacological agents. For example, CBR1 catalyzes the two-electron reduction of the C-13 carbonyl group of the anticancer anthracyclines doxorubicin and daunorubicin to generate their corresponding alcohol metabolites (doxorubicinol and daunorubicinol)(Forrest and Gonzalez, 2000). Anthracycline C-13 alcohol metabolites are cardiotoxic, have diminished tumor cell killing activities, circulate in plasma at various levels, and contribute to the unpredictable pharmacology of anthracycline drugs (Frost et al., 2002; Minotti et al., 2004). Significant interindividual variability in carbonyl reductase activity (CBR) has been documented in liver, erythrocytes, as well as in breast and lung tumors (Iwata et al., 1993; Wong et al., 1993; Rady-Pentek et al., 1997; Lopez de Cerain et al., 1999). We observed wide ranges of CBR activities in liver cytosols from black (range: 4.1 – 21.5 nmol/min·mg), and white donors (range <0.1 – 28.0 nmol/min·mg) (Covarrubias et al., 2006). However, the molecular basis of such disparities and its potential impact on CBR mediated drug metabolism remain to be elucidated. We hypothesize that interindividual differences in CBR activity may in part reflect variable rates of *CBR1* gene transcription. *CBR1* spans approximately 3.2 kb on chromosome 21 (21q22.13), contains three exons, and encodes for a monomeric 277 amino acid protein with a molecular weight of 30,375 (Wermuth et al., 1988). Notably, and in spite of the major role of CBR1 in the biotransformation of xenobiotics, there is a paucity of reports focused on the functional characterization of the human *CBR1* gene promoter. In consequence, the first aim of our study was to investigate the potential

MOL #35550

promoter activities of progressive DNA deletion constructs encompassing up to 2485 base pair (bp) of genomic sequence 5' upstream the translation start site of *CBR1* by using gene-reporter assays.

Our second aim was to test whether *CBR1* mRNA levels were induced in cell cultures incubated with prototypical activators of the nuclear glucocorticoid receptor (GR), the constitutive androstane receptor (CAR), the pregnane X receptor (PXR), and the aryl hydrocarbon receptor (AHR), respectively. We detected significant induction of *CBR1* mRNA expression in HepG2 and MCF-7 cells treated with the AHR ligand β-naphthoflavone. AHR is a ligand-activated basic helix-loop-helix transcription factor that participates in the regulation of several key mammalian genes involved in the metabolism of xenobiotics (e.g. *CYP1A1* and *CYP1B1*). After ligand binding, AHR translocates from the cytoplasm into the nucleus to form a complex with ARNT (aryl hydrocarbon receptor nuclear translocator). The resulting ligand/AHR/ARNT complex interacts with specific DNA sequences termed xenobiotic responsive elements (*XRE*) to induce the transcription of target genes (Nebert et al., 2000; Nioi and Hayes, 2004). The consensus *XRE* sequence (5'-^T/_GNGCGTG-3') contains the substitution intolerant *XRE* core motif (5'-GCGTG-3')(Lusska et al., 1993). Interestingly, we identified two perfect *XRE* motifs located at 122 bp, and 5783 bp upstream the translation start site of *CBR1* (-₁₂₂*XRE*, and -₅₇₈₃*XRE*). Therefore, our third aim was to investigate the functional impact of the proximal (-₁₂₂*XRE*), and distal (-₅₇₈₃*XRE*) *XRE* motifs by performing gene reporter assays with engineered *CBR1* promoter constructs.

The development of *Ahr* deficient mice (*Ahr*^{-/-}) has contributed to the identification of a battery of genes regulated through the AHR pathway (Fernandez-Salguero et al.,

MOL #35550

1995; Zaher et al., 1998; Sugihara et al., 2001; Jiang et al., 2004). AHR mediates the induction of several key xenobiotic metabolizing enzymes such as CYP1A1, CYP1B1, glutathione S-transferases (GST), and NQO1 (Nebert et al., 2000; Shimada et al., 2002). Thus, we extended our observations by testing whether the potent AHR ligand 2,3,7,8-tetrachlorodibenzo-p-dioxin (TCDD) induced *Cbr1* mRNA and *Cbr1* protein levels in livers from *Ahr* proficient (*Ahr*^{+/−}), and *Ahr* deficient (*Ahr*^{−/−}) mice. Together, our findings provide insights on the regulation of *CBR1*, and lay the foundation for future studies aimed toward the elucidation of the molecular bases that govern variable CBR activity in humans.

MOL #35550

MATERIALS AND METHODS

Cell culture and reagents

HepG2 (human hepatocarcinoma, HB-8065), and MCF-7 (human breast adenocarcinoma, HTB-22) cell lines were obtained from the American Type Culture Collection (Manassas, VA). Minimum essential medium (α -MEM), fetal bovine serum and other cell culture reagents were purchased from Gibco (Invitrogen, Carlsbad, CA). Cells were routinely cultured in 75 cm² vented flasks using α -MEM supplemented with 10% fetal bovine serum. Cultures were grown in an incubator at 37°C, 5% CO₂ and 95% relative humidity. Cultures were maintained at low passage numbers (n<12), and were free of mycoplasma contamination.

Dexamethasone, clotrimazole, TCPOBOP (1,4-bis-[2-(3,5-dichloropyridyloxy)]-benzene), and rifampicin were purchased from Sigma-Aldrich (St. Louis, MO). β -naphthoflavone was purchased from Indofine (Hillsborough, NJ).

Cloning of *CBR1* promoter constructs

Approximately five-kilo bases of DNA sequence upstream the translation start codon (ATG) of *CBR1* were amplified from human DNA sample HD17030 (Coriell Institute for Medical Research, Camden, NJ) by using the Expand Long Template PCR system (Roche, Indianapolis, IN). PCR primers were: 5'-CCCTGACTGCCCTTCTTA-3' (forward), and 5'-TCACCAGCGC TACATGGAT-3' (reverse). A derivative fragment of 2485 bp was cloned into a pGL3 basic luciferase vector (Promega, Fitchburg, WI), by using the following primers: 5'-GCTCTTACGCGTGCTAGCCCCGAGCTCTGAATTATCCTGAGTGG-3' (forward), and

MOL #35550

5'-CCGCGCGCCCCGTTCAGCCGAATTCATCTGCGATCTAAG-3' (reverse). Eight 5' progressive deletion constructs were made by PCR using primers listed below. The resulting products were cloned into pGL3 basic firefly luciferase reporter vectors. The identity of each construct, and the absence of cloning artifacts were verified by direct sequencing with the dye-terminator method in a 3130XL Genetic Analyzer (Applied BioSystem, Foster City, CA).

The $-_{122}XRE$ substitution intolerant core (5'-GCGTG-3') was deleted from the $-_{413}CBR1$ promoter construct using the QuickChange site directed mutagenesis kit (Stratagene, La Jolla, CA) with the following primers: 5'-CCTGCGCGCTCAGCGGCCGGTAACCCACGGGTGCGCGCCC-3', and 5'-GGGCGCGCACCCGTGGGTTACCGGCCGCTGAGCGCGCAGG-3'. Deletion of $-_{122}XRE$ was confirmed by direct sequencing analysis.

A 12 bp sequence containing the distal $-_{5783}XRE$ element (5'-TTGCGTGCCTTG-3', bases -5790 to -5779) was added to the 5` end of the $-_{2485}CBR1$ construct by using QuickChange with the following primers: 5'-CGCGTGCTAGCCTTGCCTGCCTGGAGCTCTGAATTATCC-3', and 5'-GGATAATTAGAGCTCCAAGGCACGCAAGGGCTAGCACGCG-3'. The addition of $-_{5783}XRE$ was verified by direct sequencing.

List of primers

Forward primers

$-_{1847}CBR1$: 5'-CCTAAATCTGTACTGCCAATACGCGTACAGTGACCACTAACACATGC-3'

$-_{1561}CBR1$: 5'-GAGGGAGTCACTCTGTTGACGCGTCCCAGGCTGGAGTGCAG-3'

$-_{1101}CBR1$: 5'-CCAGACCCCTCACCTGCAACGCGTGCCTGATGCCTGTTGAC-3'

MOL #35550

-746^{CBR1}: 5'-GGTACATCCTAGAGTGTACGCGTTATTGTCCGTAAAATAGGG-3'

-600^{CBR1}: 5'-CTGGCTAAGTCAGTAGCACGCGTTTGTTCATATACTTAGGGG-3'

-413^{CBR1}: 5'-CACAACTAGGAATGAACGCGTTAACAGCTGGGAG-3'

-205^{CBR1}: 5'-GCTCCGCACCCCGGACGCGTGGTCCGGTGG-3'

-101^{CBR1}: 5'-GGCGTGTAAACCCACGCGTGCGCGCCCACG-3'

Reverse primer

_{Rev}^{CBR1}: 5'- CCGCGCGCCCCGTTAGCCGAATTCTGCGATCTAAG-3'

Transient transfections and luciferase activity assays

Cells were plated 24 – 48 h before transfections in 12 well plates. Reporter gene constructs (firefly luciferase), and the SV40-driven *renilla* luciferase pRL-SV40 plasmid (Promega, Fitchburg, WI) were co-transfected into 60 - 70% confluent cell cultures by using FuGENE 6 (Roche, Indianapolis, IN). Twenty-four hours after co-transfections, cultures were washed once with phosphate buffered saline solution, and the cells were lysed with passive lysis buffer (250 µl per well) (Promega, Fitchburg, WI). Cell lysates were incubated at room temperature (15 min), mixed with a vortex blender (10 s), and centrifuged at 4°C (1500 rpm, 30 s). Luciferase reporter gene activities were determined with the Dual-Luciferase Reporter Assay System (Promega, Fitchburg, WI) according to the manufacturer's instructions. Light intensity was measured in a Synergy HT luminometer equipped with proprietary software for data analysis (BioTek, Winooski, VT). Light intensity values from cell cultures transfected with the promoter-less (pGL3) vector were used to correct for background. Corrected firefly luciferase activities were normalized to *renilla* luciferase activities and expressed as fold increases with respect to the values obtained with pGL3-basic empty vector. In all cases, three to five

MOL #35550

independent experiments were performed in duplicates to evaluate reproducibility. Unpaired Student's t-tests (two groups), and analysis of variance (ANOVA, three or more groups) were used to compare experimental means. In all cases, differences were considered to be significant at $p < 0.05$. Computations were performed with Microsoft Excel 2000 version 9.0 (Microsoft, Redmond, WA), and Sigma Plot version 8.02 (SPSS Inc, Chicago, IL).

Quantification of *CBR1* mRNA in cell cultures by real time RT-PCR

Cell cultures (70 - 80% confluence) were treated for 24 h with: dexamethasone (10 μ M), rifampicin (10 μ M), β -naphthoflavone (10 - 50 μ M), clotrimazole (20 μ M), TCPOBOP (0.250 μ M), or vehicle (DMSO). Total RNA was extracted with RNeasy Mini kit (Qiagen, Valencia, CA) according to the manufacturer's instructions. RNA was eluted with molecular biology grade water, and stored at -80°C until use. RNA concentrations were measured by spectrophotometric analysis at 260 nm in a Shimadzu UV-1601 PC spectrophotometer. Total RNA (100 ng) was reverse transcribed and amplified by using one-step QuantiTect SYBR Green RT-PCR kits (Qiagen, Valencia, CA). RT-PCR reaction mixtures were incubated on a MX4000 engine thermal cycler equipped with proprietary software for data analysis (Stratagene, La Jolla, CA). The comparative quantitation method was used to determine relative *CBR1* mRNA levels in drug-treated samples. Vehicle-treated samples were used as references, and individual β -actin mRNA levels were used as normalizers (Blanquicett et al., 2002; Bustin, 2002). *CBR1* primers were: 5'-CTGATCCCACACCCTTCAT-3' (forward) and 5'-TTAAGGGCTCTGACGCTCAT-3' (reverse); β -actin primers were: 5'-

MOL #35550

ACGGCTCCGGCATGTGCAAG-3' (forward) and 5'-TGACGATGCCGTGCTCGATG-3' (reverse). Cycling parameters for the amplifications in parallel of *CBR1* and β -actin mRNAs were: 50°C for 30 min (reverse transcription), 95°C for 10 min (Taq polymerase activation); 40 cycles of 95°C for 15 s (denaturation), 51°C for 30 s (annealing), 72°C for 30 s (extension), and 78°C for 30 s (fluorescence collection). Standard curves for *CBR1* and β -actin mRNA (10-fold dynamic range) were run in parallel to ensure accurate mRNA quantifications. In all cases, the regression coefficients (*r*) of the standard curves were *r* ≥ 0.9. Amplification efficiencies for *CBR1* and β -actin mRNAs were similar and ranged between: 125 - 175%. In all cases, experimental samples and standards for calibration curves were analyzed in quadruplicates.

Animals and treatments

Ahr^{+/-} and *Ahr^{-/-}* mice were procured from the laboratory of Dr. Christopher Bradfield (University of Wisconsin). The Institutional Animal Care and Use Committee approved the experimental protocol. Animals were housed in a temperature and humidity-controlled room under a light cycle with free access to food and water. Mice (Age: 81 ± 14 days) were treated with intraperitoneal injections of TCDD (50 µg/kg. AccuStandard Inc., New Haven, CT), or corn oil vehicle (200 µl), respectively. Animals were sacrificed by CO₂ inhalation. Livers were removed, snap-frozen in liquid nitrogen, and stored at -80°C until use.

MOL #35550

Quantification of hepatic *Cbr1* mRNA by real time RT-PCR

Liver RNA was extracted with RNeasy Mini kits (Qiagen, Valencia, CA). RNA samples (100 ng) were subjected to one step quantitative real-time RT-PCR using QuantiTect SYBR green RT-PCR kit (Qiagen, Valencia, CA). Mouse *Cbr1* primers were: 5'-ATCACTCGTGACCTGTGTCG-3' (forward), and 5'-GGTGTCGTCATTGACCTTGA-3'(reverse); β -actin primers were: 5'-GACCCAGATCATGTTGAGACCTTC-3' (forward), and 5'-GGAGTCCATCACAAATGCCAGTG-3' (reverse). Amplification conditions for murine *Cbr1* and β -actin mRNAs were: 50°C for 30 min (reverse transcription), 95°C for 10 min (Taq polymerase activation); 40 cycles of 95°C for 15 s (denaturation), 52°C for 30 s (annealing), 72°C for 30 s (extension), and 78°C for 30 s (fluorescence collection). Standard curves (10-fold dynamic range) for *Cbr1* and β -actin mRNA were run in parallel. Relative *Cbr1* mRNA levels were calculated by using the comparative quantitation method as described above. Samples were analyzed in quadruplicates.

Detection of Hepatic *Cbr1* by immunoblotting

Fragments of frozen mouse liver were homogenized in three volumes of ice-cold lysis buffer (Promega, Fitchburg, WI). The homogenates were centrifuged at 13,000g for 20 min at 4°C. The resulting supernatants (100 μ g) were separated on 4 - 20% pre-cast polyacrylamide gels (Pierce, Rockford, IL), and transferred onto Hybond ECL nitrocellulose membranes (Amersham Biosciences, Piscataway, NJ). Membranes were first incubated with a monoclonal anti human CBR1 antibody (1:1000 dilution) that cross-react with murine *Cbr1* (Abnova Corporation, Taipei City, Taiwan), and with a secondary anti-mouse IgG conjugated with horseradish peroxidase (1:1000 dilution;

MOL #35550

Amersham Biosciences, Piscataway, NJ). The membranes were also probed with anti-glyceraldehyde-3-phosphate dehydrogenase (Gapdh) antibody (1:10000 dilution; Chemicon International, Temecula, CA) to correct for differences in protein loading. Immunoreactive bands were visualized with the ECL Plus Western blotting detection system (Amersham Biosciences, Piscataway, NJ) and quantified by using a ChemiDoc XRS gel documentation system equipped with Quantity One software (BioRad, Hercules, CA).

CBR activity

Maximal CBR activity was measured in cellular lysates, and in mice liver cytosols by using the specific NAD(P)H:quinone oxidoreductase (NQO1) inhibitor dicoumarol in the presence of the substrate menadione and the NADPH cofactor (Wermuth et al., 1986; Bello et al., 2004; Covarrubias et al., 2006). Typical incubation mixtures (1 ml) contained sodium phosphate buffer (0.1 M, pH 7.4), 200 µM NADPH (Sigma-Aldrich, St. Louis, MO), 200 µM menadione (Sigma-Aldrich, St. Louis, MO), and 5 µM dicoumarol. Mixtures were equilibrated for 2 min at 37°C after the addition of cytosols (200 µg). The rates of NADPH oxidation were recorded for 4 min at 37°C in a Cary Varian Bio 300 UV-visible spectrophotometer (Palo Alto, CA). Enzymatic velocities were automatically calculated by linear regression of the $\Delta_{\text{abs}}/\Delta_{\text{time}}$ points (2,400 readings) and expressed as µmol/min.mg. Protein concentrations were determined with an assay based on Bradford's technique (BioRad, Hercules, CA).

MOL #35550

RESULTS

Cloning and functional analysis of *CBR1* promoter constructs

First, we cloned a 2485 bp DNA fragment from the 5' flanking region of *CBR1* to perform functional characterization studies. Sequencing of the insert revealed 100% identity with a segment of nucleotide sequence from locus [AP001724](#) (*Homo sapiens* genomic DNA, chromosome 21q, section 68/105; [Entrez Nucleotide Database](#)). According to the Data Base of Transcriptional Start Sites ([DBTSS](#)), *CBR1* has a predominant transcription start site (TSS, 123/146 cDNA clones) located 92 bp upstream the ATG codon (Fig. 1). Analysis of the core promoter sequence of *CBR1* revealed the presence of a typical initiator element containing the TSS (Inr, Py-Py(C)-A₊₁-N-T/A-Py-Py). The *CBR1* core promoter region has no downstream core promoter element (DPE, A/G₊₂₈-G-A/T-C/T-G/A/C), no TATA box, and no CAAT box. The core promoter is embedded in a CpG island of approximately 0.65 kb that encompasses -273 bp of 5' flanking sequence, and extends 369 bp downstream the ATG codon. There are two contiguous GC boxes located at -165 bp, and -152 bp, respectively. In addition, there is a proximal SP1 motif at -53 bp, and a relatively more distal SP1 motif embedded in the -152 bp GC box. Together, these findings indicate that the core promoter of *CBR1* has the configuration of a typical CpG island promoter (Butler and Kadonaga, 2002).

Computer assisted searches for additional cis-acting elements using the [TESS](#) and [TRANSFAC](#) databases pinpointed potential consensus motifs for a number of transcription factors including HNF-3β, IK-2, and Oct-1 (Fig. 1). We identified one proximal sequence motif for a xenobiotic response element (-₁₂₂XRE, Fig.1). Further

MOL #35550

analysis of up to 6 kb upstream the ATG codon revealed a distal *XRE* motif containing the substitution intolerant core sequence 5'-GCGTG-3' at position -5783 (-₅₇₈₃ *XRE*).

Next, we generated a series of progressive 5' deletion constructs and performed gene reporter assays in HepG2, and MCF-7 cells (Fig. 2, A and B). Results from both cell lines suggested the presence of a negative regulatory element in the -2485/-1847 region, since deletion of the 653 bp segment resulted in significant increases in luciferase activities (HepG2, Student's t test, p<0.05; MCF-7, Student's t test, p<0.05). In both cell lines, further 5' truncation of up to 746 bp resulted in no significant changes in the promoter activities of constructs -₁₈₄₇*CBR1*, -₁₅₆₁*CBR1*, and -₁₁₀₁*CBR1*, respectively (HepG2, ANOVA, p = 0.75; MCF-7, ANOVA, p = 0.83). In HepG2 cells, the -₄₁₃*CBR1* construct exerted the highest promoter activity from the series suggesting that the -600/-413 region may harbor an element whose regulatory role depend upon the cellular context. Further deletion of 208 bp (-₂₀₅*CBR1*) decreased the promoter activity in HepG2 (2.7-fold), and MCF-7 cells (2.4-fold). Data from both cell lines showed that the -205/-101 region contains cis-acting elements that are crucial to sustain gene transcription since deletion of 104 bp resulted in substantial decreases in the promoter activities by 22-fold (HepG2, Student's t test, p<0.01), and 41-fold (MCF-7, Student's t test, p<0.001), respectively. The -205/-101 segment contains two GC boxes, and the proximal -₁₂₂*XRE*. Thus, it is likely that the removal of these elements resulted in a construct (-₁₀₁*CBR1*) with diminished promoter activity (Figs. 1 and 2). In both cell lines, the -₁₀₁*CBR1* showed minimal although significant increases in transcriptional activity as compared to the pGL3-basic vector (HepG2 = 3-fold, Student's t test, p < 0.05; MCF-7 = 8-fold, Student's t test, p < 0.05). It is possible that the Inr element (-93 bp), and the

MOL #35550

proximal SP1 site (-53 bp) dictate the minimal promoter activity of the $-101 CBR1$ construct.

Induction of *CBR1* mRNA and CBR activity by a ligand of the aryl hydrocarbon receptor

To pinpoint pathways potentially involved in the transcriptional regulation of *CBR1*, we analyzed the effect of different receptor activators on *CBR1* mRNA levels. Cultures of HepG2 cells were incubated with different receptor activators at concentrations known to affect the regulation of other drug metabolizing enzymes (Schuetz et al., 1993; Zhang et al., 2003; Hempel et al., 2004). *CBR1* and β -actin (normalizer) mRNA levels were determined simultaneously by quantitative real-time RT-PCR (see Materials and Methods). We detected no changes in *CBR1* mRNA levels after incubations with the GR agonist dexamethasone. Similarly, incubations with activators of CAR (clotrimazole and TCPOBOP), and PXR (rifampicin) did not significantly affect *CBR1* mRNA levels. In contrast, incubations with the prototypical AHR ligand β -naphthoflavone (50 μ M, 24 h) induced *CBR1* mRNA levels by 5.5-fold (Student's t test, $p<0.005$), as compared to controls (Fig. 3). In MCF-7 cells, β -naphthoflavone exerted moderate cytotoxicity ($\approx 20 - 30\%$) at the 50 μ M concentration, whereas incubations with 10 μ M resulted in negligible cytotoxicity ($\leq 5\%$), and induced *CBR1* mRNA by 2.5-fold (Student's t test, $p<0.05$. Fig. 3). The increase in *CBR1* mRNA levels in MCF-7 cells treated with β -naphthoflavone was paralleled by a 3-fold increase in maximal cytosolic CBR activity ($CBR_{\text{controls(DMSO)}}: 50 \pm 13 \text{ pmol/min.mg}$ vs. $CBR_{\beta\text{-naphthoflavone}}: 140 \pm 2 \text{ pmol/min.mg}$).

MOL #35550

Transcriptional activation of *CBR1* promoter constructs by β -naphthoflavone

Next, we tested whether β -naphthoflavone induced the gene reporter activities of different *CBR1* promoter constructs encompassing up to 1561 bp of 5' flanking region. In all cases, incubations with β -naphthoflavone (10 μ M, 48h) or vehicle (DMSO) were performed 24 h after the co-transfections with reporter constructs (see Materials and Methods). On average, β -naphthoflavone induced the luciferase activities of the constructs by 11- ($_{-1561}CBR1$, $p<0.05$), 5- ($_{-600}CBR1$, $p<0.05$), and 15-fold ($_{-413}CBR1$, $p<0.001$), in MCF-7 cells as compared to vehicle treated controls (Fig. 4).

Functional *XRE* motifs in the promoters of drug-metabolizing enzymes are necessary to activate gene transcription in response to AHR ligands (Nioi and Hayes, 2004). Thus, we first tested whether the $_{-122}XRE$ motif was necessary to induce luciferase reporter gene expression in the presence of the ligand β -naphthoflavone. The removal of $_{-122}XRE$ decreased the β -naphthoflavone response by 9-fold in MCF-7 cells (Student's t test $p<0.001$. Fig. 5).

In another set of experiments, we evaluated the ability of the distal $_{-5783}XRE$ to augment reporter gene activity in response to β -naphthoflavone. To achieve this end, a 12 bp sequence (bases: -5790 to -5779) containing the $_{-5783}XRE$ was fused into the $_{-2485}CBR1$ reporter construct. Treatment with β -naphthoflavone increased the reporter activity of $_{-2485}CBR1$ by 4-fold as compared to incubations with the vehicle DMSO (Student's t test, $p<0.05$). Fusion of the distal $_{-5783}XRE$ to $_{-2485}CBR1$ further enhanced the β -naphthoflavone response by 5-fold (Student's t test, $p<0.0001$. Fig. 6).

MOL #35550

Induction of hepatic *Cbr1* by TCDD treatment in *Ahr^{+/-}* and *Ahr^{-/-}* mice

We extended our observations by evaluating whether the administration of the potent AHR ligand TCDD impacted on the expression of *Cbr1* in livers from *Ahr^{+/-}* and *Ahr^{-/-}* mice. First, TCDD (50 µg/kg) was administered by a single intraperitoneal injection, and the expressions of *Cbr1* mRNA and protein were analyzed from livers collected 72 h after treatments. In heterozygous *Ahr^{+/-}* animals, TCDD treatment resulted in a 2-fold induction of *Cbr1* mRNA levels as compared to vehicle treated heterozygous controls. In contrast, TCDD treatment failed to induce the expression of hepatic *Cbr1* mRNA in homozygous null (*Ahr^{-/-}*) mice (Fig. 7, A and B). Notably, the induction of hepatic *Cbr1* mRNA in heterozygous *Ahr^{+/-}* animals treated with TCDD was paralleled by a 2-fold increase in *Cbr1* protein levels as determined by semi-quantitative immunoblotting (Fig. 7, C, D, E and F). In line, hepatic Cbr activity increased by 40% in TCDD-treated mice with one active *Ahr* allele (*Ahr^{+/-}*), whereas the levels of Cbr activity remained essentially unchanged in the livers of TCDD-treated *Ahr^{-/-}* mice (data not shown). Moreover, Cbr activity was induced by 5-fold in livers of *Ahr^{+/+}* mice treated with three consecutive doses of TCDD (50 µg/kg/day X 3 days) as compared to vehicle treated animals ($p < 0.05$. Fig. 8, A). Identical TCDD treatments failed to induce hepatic Cbr activity in *Ahr^{-/-}* mice ($p = 0.32$. Fig. 8, B).

MOL #35550

DISCUSSION

The first aim of our study was to perform the functional characterization of the promoter of human *CBR1*. Our sequence annotation showed that the core promoter of *CBR1* has the features of a prototypical CpG promoter including two GC boxes, proximal SP1 sites, and the absence of TATA and DPE elements (Fig. 1). In humans, about half of the promoter regions are located in CpG islands, and gene transcription may occur at different start sites (Butler and Kadonaga, 2002). In line, *CBR1* has a predominant start site at -92 bp, and 16% of the clones reported in [DBTSS](#) showed alternative start sites (e.g. -101 bp, and -125 bp). Our results from gene reporter experiments in HepG2 and MCF-7 cells demonstrated the presence of regulatory regions that appear to be relevant to promote transcription under basal conditions in both cell types. For example, deletion of the segment that contains the two GC boxes, and the proximal $-122XRE$ (-205/-101) significantly reduced the reporter gene activity of the $-205CBR1$ construct as compared to the $-413CBR1$ construct in HepG2 (22-fold), and MCF-7 (41-fold) cells. It has been demonstrated that SP1 binding sites together with an Inr motif can activate transcription in CpG promoters (Smale and Baltimore, 1989; Butler and Kadonaga, 2002). Consequently, the *CBR1* -101/+1 region harboring both SP1 and Inr consensus displayed minimal although significant promoter activities in both cell lines. Functional mutagenesis analysis within the context of the minimal *CBR1* promoter will provide further evidence on the role of the Inr and SP1 elements.

The second aim of this study was to evaluate the ability of prototypical receptor activators to induce the expression of *CBR1* mRNA. In agreement with the seminal observation by Forrest et al., the AHR ligand β -naphthoflavone was the only compound

MOL #35550

that significantly induced *CBR1* mRNA levels in HepG2, and MCF-7 cells (Forrest et al., 1990). Furthermore, our data with engineered reporter constructs suggest that $-_{122}XRE$, and $-_{5697}XRE$ may act as *bona fide* functional elements to activate AHR mediated gene transcription in the presence of AHR ligands.

The overall identity between the human *CBR1* proximal promoter region (\approx 600 bp) and the mouse *Cbr1* putative promoter region is 33% (global alignment analysis). Similar overall identity values (\approx 36%) were obtained when comparisons were extended up to 2500 bp. Further analysis by using the sequence comparison tool from [DBTSS](#) pinpointed 3 DNA fragments (size range: 38 - 42 bp) with relatively high sequence identity values (average: 72%). In addition, we identified a proximal *XRE*, and a GC box element on the murine sequence that correspond with similar motifs on the human *CBR1* promoter (Fig. 9). Sun et al. analyzed the positional conservation of *XRE* core motifs between several murine and human genes, and found that only 39% of the human-mouse orthologs contain positionally conserved *XREs* (Sun et al., 2004). Thus, the positional conservation of the substitution intolerant *XRE* core in both murine and human *CBR1* sequences is interesting, and supports the notion that the transcription of *CBR1* in both species is controlled by similar key regulatory factors (e.g. AHR). Furthermore, our experiments with heterozygous *Ahr^{+/−}* and homozygous *Ahr^{−/−}* mice clearly showed that *Ahr* plays a pivotal role in mediating *Cbr1* induction *in vivo*. Notably, the presence of one active *Ahr* allele was essential to induce *Cbr1* mRNA, *Cbr1* protein, and *Cbr* activity in *Ahr^{+/−}* mice treated with the AHR ligand TCDD. In contrast, TCDD treatment failed to induce *Cbr1* expression in homozygous null animals (*Ahr^{−/−}*).

MOL #35550

The reduction of carbonyl moieties catalyzed by CBR1 is an important step in the metabolism of a wide variety of clinically relevant drugs such as the anticancer daunorubicin, the antipsychotic haloperidol and the antidiabetic acetohexamide (Ohara et al., 1995; Forrest and Gonzalez, 2000; Rosemond and Walsh, 2004). CBR1 also catalyzes the reduction of toxins such as the potent tobacco carcinogen 4-methylnitrosamino-1-(3-pyridyl)-1-butanone (NNK). In humans, NNK is detoxified through 2-electron reductions catalyzed mainly by cytosolic CBR1 and microsomal 11 β -hydroxysteroid dehydrogenase type I (11 β -HSD1). The resulting alcohol metabolite 4-methylnitrosamino-1-(3-pyridyl)-1-butanol (NNAL) can be further subjected to glucuronidation to form NNAL-glucuronide, which is excreted in urine (Maser et al., 2000). Variable *CBR1* mRNA expression has been described in human lung, and a recent study on 59 non-small cell lung carcinoma patients reported higher post-operative survival rates among patients having tumors containing “high” *CBR1* mRNA expression as compared to those with tumors presenting “low” *CBR1* mRNA expression (5-year survival *CBR1*-high: 68.3% vs. 5-year survival *CBR1*-low: 36.5%, $p = 0.03$) (Finckh et al., 2001; Takenaka et al., 2005). The polycyclic aromatic hydrocarbon benzo(a)pyrene (BP) is one of the best-characterized carcinogens in cigarette smoke, and is also a powerful AHR ligand (Denison and Nagy, 2003). Moreover, BP induces *Cbr1* expression significantly in *Ahr* proficient mice but fails to induce *Cbr1* in *Ahr* deficient animals (Lakhman, Schuetz and Blanco, unpublished observations). Thus, it is reasonable to hypothesize that BP may modulate *CBR1* expression in the lungs of smokers via the AHR pathway, which in turn impacts on the CBR1-mediated

MOL #35550

detoxification of other smoke carcinogens relevant to the pathogenesis of lung cancer such as NNK.

In conclusion, our results describe the first functional characterization of the promoter of human *CBR1*, and indicate that AHR is a key mediator in dictating variable CBR activity.

ACKNOWLEDGEMENTS

The authors gratefully acknowledge the excellent assistance of Dr. Lubin Lan.

MOL #35550

REFERENCES

- Bello RI, Gomez-Diaz C, Navas P and Villalba JM (2004) NAD(P)H:quinone oxidoreductase 1 expression, hydrogen peroxide levels, and growth phase in HeLa cells. *Methods Enzymol* 382:234-243.
- Blanquicett C, Johnson MR, Heslin M and Diasio RB (2002) Housekeeping gene variability in normal and carcinomatous colorectal and liver tissues: applications in pharmacogenomic gene expression studies. *Anal Biochem* 303:209-214.
- Bustin SA (2002) Quantification of mRNA using real-time reverse transcription PCR (RT-PCR): trends and problems. *J Mol Endocrinol* 29:23-39.
- Butler JEF and Kadonaga JT (2002) The RNA polymerase II core promoter: a key component in the regulation of gene expression. *Genes Dev.* 16:2583-2592.
- Covarrubias VG, Lakhman SS, Forrest A, Relling MV and Blanco JG (2006) Higher activity of polymorphic NAD(P)H:quinone oxidoreductase in liver cytosols from blacks compared to whites. *Toxicol Lett* 164:249-258.
- Denison MS and Nagy SR (2003) Activation of the aryl hydrocarbon receptor by structurally diverse exogenous and endogenous chemicals. *Annu Rev Pharmacol Toxicol* 43:309-334.
- Fernandez-Salguero P, Pineau T, Hilbert DM, McPhail T, Lee SS, Kimura S, Nebert DW, Rudikoff S, Ward JM and Gonzalez FJ (1995) Immune system impairment and hepatic fibrosis in mice lacking the dioxin-binding Ah receptor. *Science* 268:722-726.
- Finckh C, Atalla A, Nagel G, Stinner B and Maser E (2001) Expression and NNK reducing activities of carbonyl reductase and 11beta-hydroxysteroid dehydrogenase type 1 in human lung. *Chem Biol Interact* 130-132:761-773.
- Forrest GL, Akman S, Krutzik S, Paxton RJ, Sparkes RS, Doroshow J, Felsted RL, Glover CJ, Mohandas T and Bachur NR (1990) Induction of a human carbonyl reductase gene located on chromosome 21. *Biochim Biophys Acta* 1048:149-155.
- Forrest GL and Gonzalez B (2000) Carbonyl reductase. *Chem Biol Interact* 129:21-40.
- Frost BM, Eksborg S, Bjork O, Abrahamsson J, Behrendtz M, Castor A, Forestier E and Lonnerholm G (2002) Pharmacokinetics of doxorubicin in children with acute

MOL #35550

lymphoblastic leukemia: multi-institutional collaborative study. *Med Pediatr Oncol* 38:329-337.

Hempel N, Wang H, LeCluyse EL, McManus ME and Negishi M (2004) The human sulfotransferase SULT1A1 gene is regulated in a synergistic manner by Sp1 and GA binding protein. *Mol Pharmacol* 66:1690-1701.

Iwata N, Inazu N, Hara S, Yanase T, Kano S, Endo T, Kuriwa F, Sato Y and Satoh T (1993) Interindividual variability of carbonyl reductase levels in human livers. *Biochem Pharmacol* 45:1711-1714.

Jiang W, Welty SE, Couroucli XI, Barrios R, Kondraganti SR, Muthiah K, Yu L, Avery SE and Moorthy B (2004) Disruption of the Ah receptor gene alters the susceptibility of mice to oxygen-mediated regulation of pulmonary and hepatic cytochromes P4501A expression and exacerbates hyperoxic lung injury. *J Pharmacol Exp Ther* 310:512-519.

Lopez de Cerain A, Marin A, Idoate MA, Tunon MT and Bello J (1999) Carbonyl reductase and NADPH cytochrome P450 reductase activities in human tumoral versus normal tissues. *Eur J Cancer* 35:320-324.

Lusska A, Shen E and Whitlock JP, Jr. (1993) Protein-DNA interactions at a dioxin-responsive enhancer. Analysis of six bona fide DNA-binding sites for the liganded Ah receptor. *J Biol Chem* 268:6575-6580.

Maser E, Stinner B and Atalla A (2000) Carbonyl reduction of 4-(methylnitrosamino)-1-(3-pyridyl)-1-butanone (NNK) by cytosolic enzymes in human liver and lung. *Cancer Lett* 148:135-144.

Minotti G, Menna P, Salvatorelli E, Cairo G and Gianni L (2004) Anthracyclines: Molecular Advances and Pharmacologic Developments in Antitumor Activity and Cardiotoxicity. *Pharmacol Rev* 56:185-229.

Nebert DW, Roe AL, Dieter MZ, Solis WA, Yang Y and Dalton TP (2000) Role of the aromatic hydrocarbon receptor and [Ah] gene battery in the oxidative stress response, cell cycle control, and apoptosis. *Biochem Pharmacol* 59:65-85.

Nioi P and Hayes JD (2004) Contribution of NAD(P)H:quinone oxidoreductase 1 to protection against carcinogenesis, and regulation of its gene by the Nrf2 basic-region leucine zipper and the arylhydrocarbon receptor basic helix-loop-helix transcription factors. *Mutation Research/Fundamental and Molecular Mechanisms of Mutagenesis* 555:149-171.

MOL #35550

- Ohara H, Miyabe Y, Deyashiki Y, Matsuura K and Hara A (1995) Reduction of drug ketones by dihydrodiol dehydrogenases, carbonyl reductase and aldehyde reductase of human liver. *Biochem Pharmacol* 50:221-227.
- Rady-Pentek P, Mueller R, Tang BK and Kalow W (1997) Interindividual variation in the enzymatic 15-keto-reduction of 13,14-dihydro-15-keto-prostaglandin E1 in human liver and in human erythrocytes. *Eur J Clin Pharmacol* 52:147-153.
- Rosemond MJ and Walsh JS (2004) Human carbonyl reduction pathways and a strategy for their study in vitro. *Drug Metab Rev* 36:335-361.
- Schuetz EG, Schuetz JD, Strom SC, Thompson MT, Fisher RA, Molowa DT, Li D and Guzelian PS (1993) Regulation of human liver cytochromes P-450 in family 3A in primary and continuous culture of human hepatocytes. *Hepatology* 18:1254-1262.
- Shimada T, Inoue K, Suzuki Y, Kawai T, Azuma E, Nakajima T, Shindo M, Kurose K, Sugie A, Yamagishi Y, Fujii-Kuriyama Y and Hashimoto M (2002) Arylhydrocarbon receptor-dependent induction of liver and lung cytochromes P450 1A1, 1A2, and 1B1 by polycyclic aromatic hydrocarbons and polychlorinated biphenyls in genetically engineered C57BL/6J mice. *Carcinogenesis* 23:1199-1207.
- Smale ST and Baltimore D (1989) The "initiator" as a transcription control element. *Cell* 57:103-113.
- Sugihara K, Kitamura S, Yamada T, Ohta S, Yamashita K, Yasuda M and Fujii-Kuriyama Y (2001) Aryl hydrocarbon receptor (AhR)-mediated induction of xanthine oxidase/xanthine dehydrogenase activity by 2,3,7,8-tetrachlorodibenzo-p-dioxin. *Biochem Biophys Res Commun* 281:1093-1099.
- Sun YV, Boverhof DR, Burgoon LD, Fielden MR and Zacharewski TR (2004) Comparative analysis of dioxin response elements in human, mouse and rat genomic sequences. *Nucleic Acids Res* 32:4512-4523.
- Takenaka K, Ogawa E, Oyanagi H, Wada H and Tanaka F (2005) Carbonyl Reductase Expression and Its Clinical Significance in Non-Small-Cell Lung Cancer. *Cancer Epidemiol Biomarkers Prev* 14:1972-1975.
- Wermuth B, Bohren KM, Heinemann G, von Wartburg JP and Gabbay KH (1988) Human carbonyl reductase. Nucleotide sequence analysis of a cDNA and amino acid sequence of the encoded protein. *J Biol Chem* 263:16185-16188.

MOL #35550

Wermuth B, Platts KL, Seidel A and Oesch F (1986) Carbonyl reductase provides the enzymatic basis of quinone detoxication in man. *Biochem Pharmacol* 35:1277-1282.

Wong JM, Kalow W, Kadar D, Takamatsu Y and Inaba T (1993) Carbonyl (phenone) reductase in human liver: inter-individual variability. *Pharmacogenetics* 3:110-115.

Zaher H, Yang TJ, Gelboin HV, Fernandez-Salguero P and Gonzalez FJ (1998) Effect of phenobarbital on hepatic CYP1A1 and CYP1A2 in the Ahr-null mouse. *Biochem Pharmacol* 55:235-238.

Zhang S, Qin C and Safe SH (2003) Flavonoids as aryl hydrocarbon receptor agonists/antagonists: effects of structure and cell context. *Environ Health Perspect* 111:1877-1882.

MOL #35550

FOOTNOTES

This work was supported by NIH/NIGMS grant R01GM73646 to J.G.B., and NIH/NIGMS grant R01GM60346 to E.G.S.

MOL #35550

FIGURE LEGENDS

Figure 1

Annotated sequence from the 5' flanking region of human *CBR1*. The transcription start site (-92 bp, DBTSS) is indicated with a solid arrow, and the Inr element is underlined. The different fragments corresponding to the series of deletion promoter constructs are indicated with dotted arrows. The proximal *XRE* motif ($-122XRE$) is indicated in a grey box, and putative transcription factor binding sites are indicated in clear boxes. Abbreviations: AP1, activator protein 1; HINF A, histone nuclear factor A; SP1, specificity protein 1; SF1, steroidogenic factor 1; NF-Kappa B, Nuclear factor kappa B; Oct 1, octamer-binding transcription factor; CAC, CACCC binding protein; Ik-2, Ikaros 2 protein; GATA, GATA or GATAA sequence; HNF 3 β , hepatic nuclear factor 3 β ; YY1, Yin Yang 1.

Figure 2

Functional analysis of human *CBR1* promoter constructs in HepG2 cells (panel A), and MCF-7 cells (panel B). Panels show schematic representations of each *CBR1* promoter construct (left), and its corresponding luciferase activity from gene reporter experiments (right). Luciferase activities were measured as described in Materials and Methods. Light intensity values from transfections with the promoter-less vector were used to correct for background. Corrected luciferase activity values were normalized to *renilla* luciferase activity and expressed as fold increases with respect to the values obtained with pGL3-basic empty vector. Each value represents the mean \pm SD of four independent experiments performed in duplicates.

Figure 3

Induction of *CBR1* mRNA in HepG2 cells (panel A), and MCF-7 cells (panel B) by prototypical receptor activators. HepG2 cells were incubated with: vehicle (DMSO, 0.01%), dexamethasone (10 μ M), β -naphthoflavone (50 μ M), clotrimazole (20 μ M), TCPOBOP (0.250 μ M), and rifampicin (10 μ M) for 24 h. MCF-7 cells were incubated

MOL #35550

with vehicle (DMSO, 0.01%), and β -naphthoflavone (10 μ M) for 24 h. The expression of *CBR1* mRNA was analyzed by quantitative real-time RT-PCR using specific primers as described in Materials and Methods. Each value represents the mean \pm SD from three independent experiments analyzed in quadruplicates. Asterisks indicate significant differences from the *CBR1* mRNA levels from vehicle treated cells (*, p<0.005; **, p<0.05).

Figure 4

Effect of the AHR ligand β -naphthoflavone on the gene reporter activities of *CBR1* promoter constructs. Cultures of MCF-7 cells were co-transfected with *CBR1* reporter constructs (-₁₅₆₁*CBR1*, -₆₀₀*CBR1* and -₄₁₃*CBR1*), and the normalizer plasmid pRL-SV40. Twenty-four hours after co-transfections, cells were treated with β -naphthoflavone (10 μ M) or vehicle (DMSO, 0.01%) for 48 h. Luciferase activities were measured as described in Materials and Methods. For each construct, normalized luciferase activities were expressed as fold increases with respect to the values from control incubations, which were set arbitrarily at 1. Data represent the mean \pm SD from three independent experiments performed in duplicates. Asterisks indicate significant difference from vehicle treated cells (*, p<0.05; **, p<0.05; ***, p<0.001).

Figure 5

Effect of β -naphthoflavone on the gene reporter activities of the promoter constructs -₄₁₃*CBR1*, and -₄₁₃*CBR1*- Δ -₁₂₂*XRE*. Co-transfections included the normalizer construct (pRL-SV40), and: a) the intact -₄₁₃*CBR1* construct, or b) the engineered -₄₁₃*CBR1*- Δ -₁₂₂*XRE* construct (without -₁₂₂*XRE* motif). Twenty-four hours after co-transfections, cells were treated with β -naphthoflavone (10 μ M) or vehicle (DMSO, 0.01%) for 48 h. Luciferase activities were measured as described in Materials and Methods. For each construct, normalized luciferase activities were expressed as fold increases with respect to the values from control incubations (DMSO), which were set arbitrarily at 1. Data represent the mean \pm SD from three independent experiments performed in duplicates.

MOL #35550

The asterisk indicates significant difference from the luciferase activity exerted by the -₄₁₃CBR1 construct in the presence of β-naphthoflavone (*, p<0.001).

Figure 6

Effect of β-naphthoflavone on the gene reporter activities of -₂₄₈₅CBR1, and -₂₄₈₅CBR1+₋₅₇₈₃XRE. Both constructs are schematized at the top of the graph. Co-transfections included the normalizer construct (pRL-SV40), and: a) the intact -₂₄₈₅CBR1 construct, or b) the engineered -₂₄₈₅CBR1+₋₅₇₈₃XRE construct. Twenty-four hours after co-transfections, cells were treated with β-naphthoflavone (10 μM) or vehicle (DMSO, 0.01%) for 48 h. Luciferase activities were measured as described in Materials and Methods. For each construct, normalized luciferase activities were expressed as fold increases with respect to the values from control incubations, which were set arbitrarily at 1. Data represent the mean ±SD from three independent experiments performed in duplicates. Asterisks indicate significant difference from vehicle treated cells (*, p<0.05; **, p < 0.0001).

Figure 7

Effect of TCDD on Cbr1 mRNA, and Cbr1 protein expression in livers from Ahr^{+/−}, and Ahr^{−/−} mice. Hepatic Cbr1 mRNA levels in Ahr^{+/−} (panel A), and Ahr^{−/−} (panel B) mice treated with vehicle (n = 2), or TCDD (n = 2), respectively. The expression of Cbr1 mRNA was analyzed by using specific primers as described in Materials and Methods. Bars represent the mean ±SD from two quantifications performed in quadruplicates for each animal. Immunodetection of hepatic Cbr1 in Ahr^{+/−} (panel C), and Ahr^{−/−} mice (panel E). Hepatic Cbr1 and Gapdh were detected with specific antibodies as described in Materials and Methods. Immunoreactive bands were visualized in a ChemiDoc XRS gel documentation system. The intensities from the immunoreactive Gapdh bands were used to correct for differences in protein loading during densitometric analyses. Densitometric analyses of Cbr1 in livers from Ahr^{+/−} (panel D), and Ahr^{−/−} mice (panel F).

MOL #35550

Each bar represent the level of Cbr1 expressed as fold induction with respect to the average intensity value obtained from vehicle treated animals.

Figure 8

Effect of TCDD on hepatic Cbr activity in heterozygous *Ahr^{+/−}* (panel A), and homozygous *Ahr^{−/−}* (panel B) mice. Each bar represents the average from two measurements performed in duplicates. Insets show hepatic Cbr activity expressed as fold induction with respect to the average activity value obtained from vehicle treated animals.

Figure 9

DNA sequence alignment of the human and mice *CBR1* 5' flanking regions. Sequences were aligned by using the global positioning alignment algorithm (GAP). XRE core motifs and GC-boxes are highlighted in grey.

Figure 1

► -2485
GAGCTCTGAATTATCCTGAGTGGAAAAAAACCAAAAACAAACTACAAACTGTATGACTCCATCTATGTAACATTT -2485 T0 -2402
HNF A
TTGAAACAAACAACTTGT **AGAATTC** GTAACAGATTAGTGGTTGCCATGAATTAGAGTTGGTTGGAGTAACAGAGAGT -2401 T0 -2320
GATA-1
ATGTTTGGT **GATAAA** AGTGCACAGGAGGGCTTTGTGCTAATAGAAACATTTCACTATAGGGTGGATACACAA -2319 T0 -2238
GATA-1
ACCAACATT **GATAAA** ATTATATAGGACTAAATACATACACAAAGTACACATCAAACGGGAAATCTGAGTATGATTGGT -2237 T0 -2156
GAATGTTTGTGTCATATCTTCACTGTGATGTTGACTATCTTCAATATGTTACTATTGAGTGAATGAGTAAAGG -2155 T0 -2074
GTAAGGAATCTCTGTATTATTCCTAACTGCATGTGACTCTATAATTAGCTGACAAAAATTTCAGTTGAAATGAAAGCAA -2073 T0 -1992
GGGTCTTCCTTGATTATTAACCTGTTAAAGCAACTGATTGGAAACCTACCTGAAATTGCAATGTAATTGCAATCTATT -1991 T0 -1910
NF-KappaB ► -1847 :
TAAAGCAGTGGTGTCAACAGACCTTCTGCAAGGAT **GGAAATTC** CAAATCTGTACTGCCAAATACAGTGACCACTAACAA -1909 T0 -1828
CATGCACATATTGAGCACTGGAGATGTGGCTAGTGCACACTAAAAAACTGAATTACAAATTGCTTAATTGAAATTATGTT -1827 T0 -1746
HNF A YY1 delta factor
TAAATGCCACCTGTGATAGTGGCACCTATGGGACAGCAC **AGAATTC** AAACCTGACCTTATTCCTATTCCCTGTAAGTA -1745 T0 -1664
GGAAGGAGGAACACTCACTTGAACCATGCATTGTCCCCTAGGACAGATGTTATGGCTCTTTTTCTTTCTTTT -1663 T0 -1582
AP1-1561 ►
TTTTTGAGAC **GGACTCA** CTCAGTTGCCAGGCTGGAGTGCAGTGGCATGATCTCGGCTCGCTGAAACCTCCGCTCTGGGG -1581 T0 -1500
TTCAAGCAAGCAATTCTCTGCTTCAGCCTCCCAAGTAGCTGGATTACAGGCGCCTGCCACACACCCAGCTAATTTGTA -1499 T0 -1418
CREB/Oct1
TTTTTTTTTTTTTTTTTTAGTAGAGATGGGTTTACCATCTTGGCCAGGCTGGTCTTGAACTCC **TGACCTCA** TGA -1417 T0 -1336
TCCACCCACCTCAGCCTCCAAAGTGTGAGATTACAGGCGTGGCACCAGCCTGGCTCTTTGAATAAACAAA -1335 T0 -1254
TTGACCCCTCCAGTCTAAAAACTGAGAAATTACATTGCTTATCTGAGTTCTTCTCAGGGAACTAGCCATCAGTCCT -1253 T0 -1172
GATA-1 ► -1101 :
CCCGAGATAACGACCAAGGAACCTGAAACTTATCGGATCACCATCTGGAAAATCAGACACCAAGACCCCTCACCTGCAACAATT -1171 T0 -1090
GCCTGATGCCCTGTTGACCCACTCCTCTTCATCTCTCCCTAACCTCTGCTATTTCACATGCAAGTTACATTCTTCCCTGC -1089 T0 -1008
AP-1
TATATCCTAATT **TTAAATCA** GTTGAGAAGATGATTTGAGACTGATCTCTCCCTCTAGGCTGTAGCACCCAAATAATGCCTT -1007 T0 -926
CTTCCCTGACAATAATGGGTCTCAGTGAATGGCTTCTGTGCTGTGAACCACCAAGACCTAGACCAAAACTCCTGGCATTCT -925 T0 -844
CTAACAAATTCCACCAACTGAACTAAGTTAAATTCTGAGGATGGATCCCTGTTCTCATTAAAGATGGGATTAAAAG -843 T0 -762
-746 :
GATA-1
GTACATCCTAGAGTGTATTGTCCTGTAAATAGGGCTGTGAAACCCCTACACCTATGCAAC **CATTA** CTGATGCCCTGC -761 T0 -680
-600 :
AAATGCCAGAGAAGTAACCTTATAAAGATTAGTGAATGTTCCCACCAATTATTGAAAATCTGGCTAAGTCAGTAGCTT -679 T0 -598
SF-1
GTTTCACTACTTACGGGGAAATCAACAAAAACTGATGCCCTGTTATTCCCT **TCCAGT** TTCTCTGCAACTCTAGCTCC -597 T0 -516
HNF-3β GATA-1 Oct-1
AAAGACTGCAGTCC **TGCACTATTTTT** TTTT **AGATA** ACACAGGAAAAAGAAAAACCTGCAATGCAATGTACTATTTC -515 T0 -434
-413 :
IK-2
TTCAAAACACAACCTAGGAATGTTGAAC **AGCTGGGAGAT** ATGAAGAAACCCCTAGAGAACCAAGGGCAAGCAGTGAGTTC -433 T0 -352
E-BOX
AGATCTAGGCACATGGCACTAGGAATGGTTCTCACTGC **CACGTG** GGCAAGCAACAGCCAGTAGAGACCAAGCCTCGG -351 T0 -270
-205 :
CAC-Binding protein
TCTTCGGCCTGCGGTTCTGCAAGTCAGGCTAGCTGGCTCCGCTGCTCCGACCCGGAGGGTCC **GGGGGGGG** AGGG -269 T0 -188
GC-BOX SP1/GC BOX XRE
GTAGGGATGGTTCTGCCCGCCCCGCT **AGGGCGGGG** CTGCCTGCGCGCTCAGCGGCCGG **GGTG** TAACCCACGGGTGCG -187 T0 -106
-101 :
Inr ► SP1
CGCCCAACGACCGCC **AGACTC** GAGCAGTCTCTGGAACCAAGCTGCGGGGCT **TCCCG** GGCGCTGAGCCAGGTCTGTTCTCACCGCAG -105 T0 -24
-1
GTGTTCCGCGCGCCCCGTTCAAGCC **ATG** -23 T0 +3

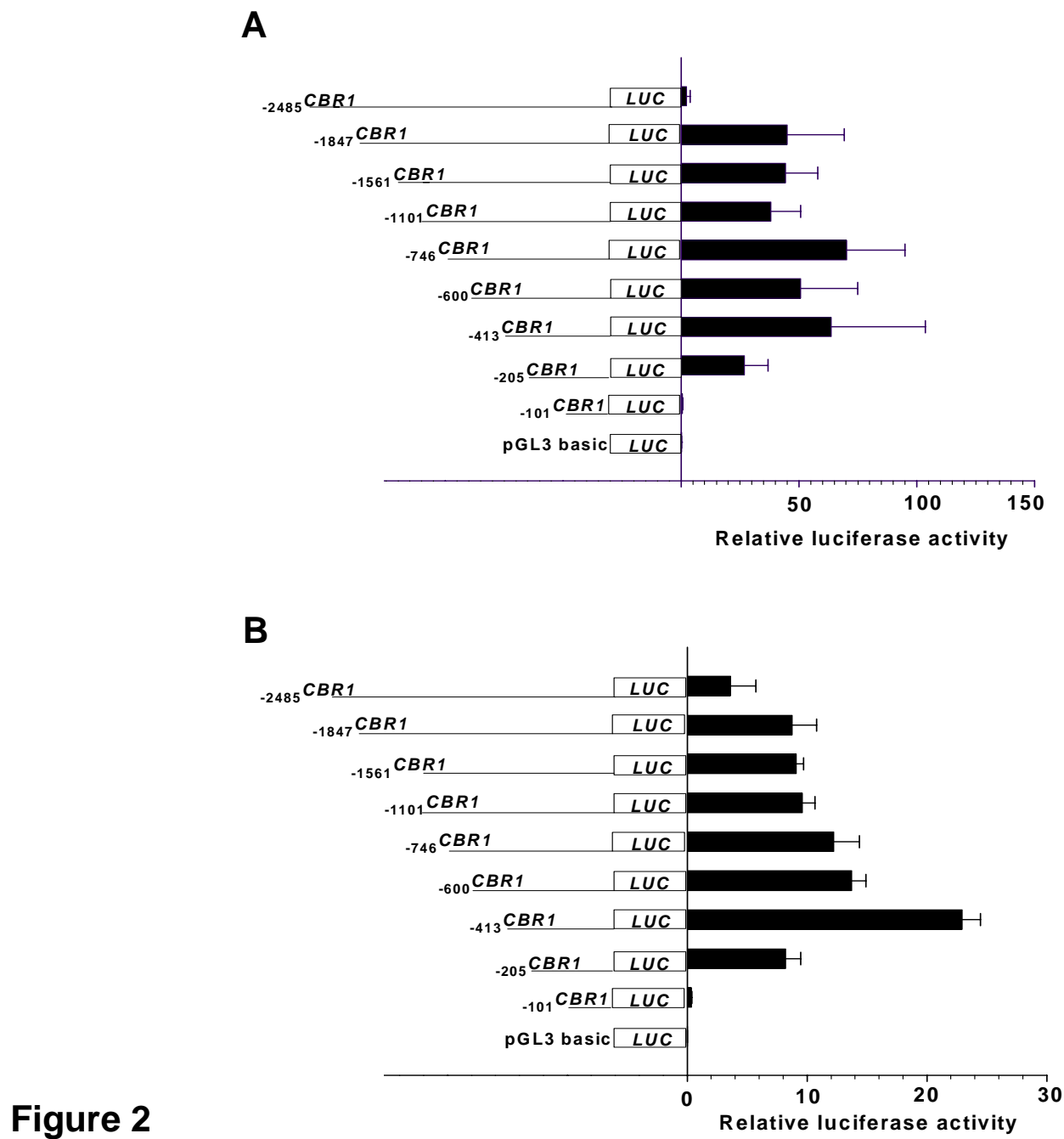


Figure 2

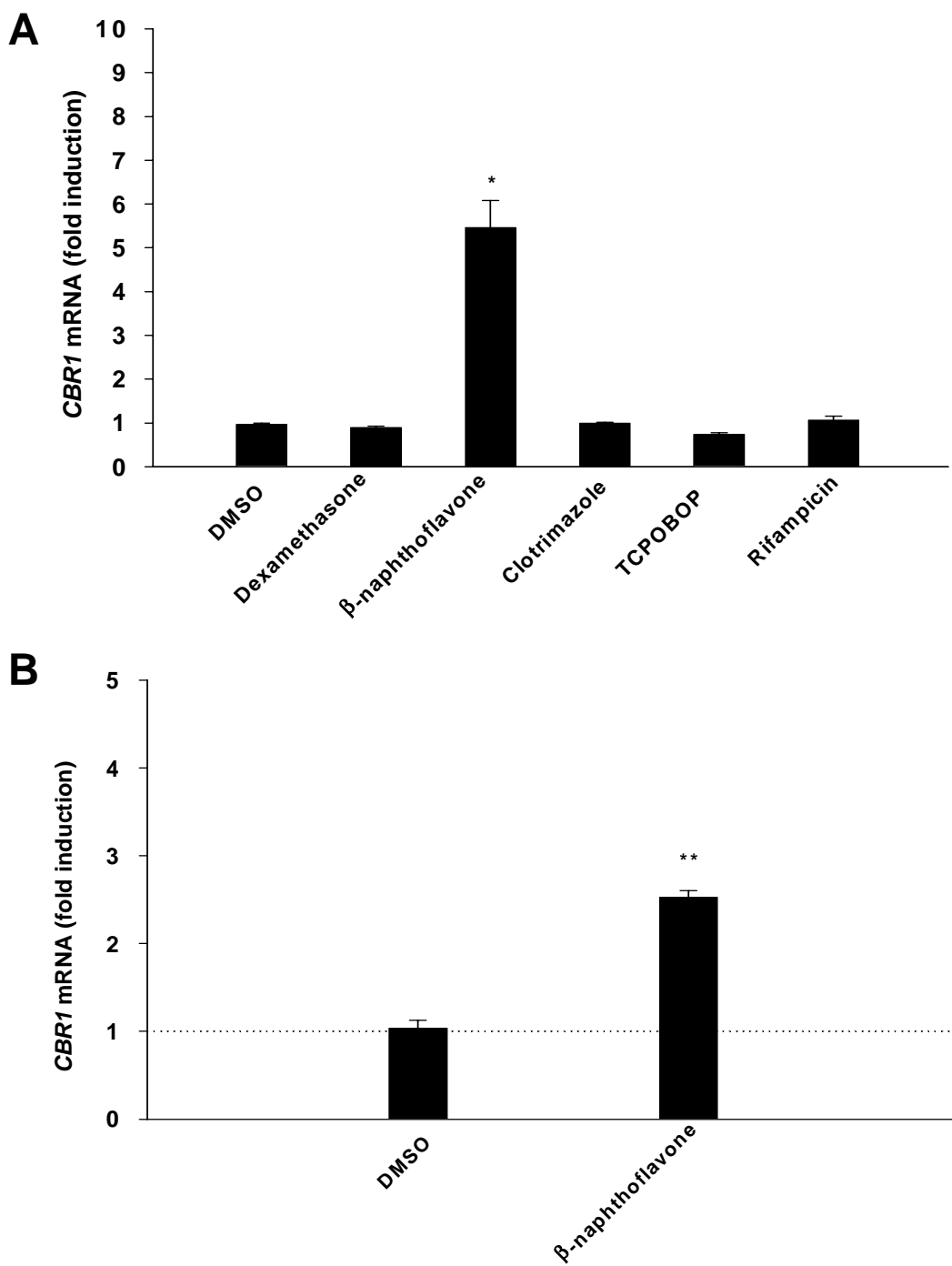


Figure 3

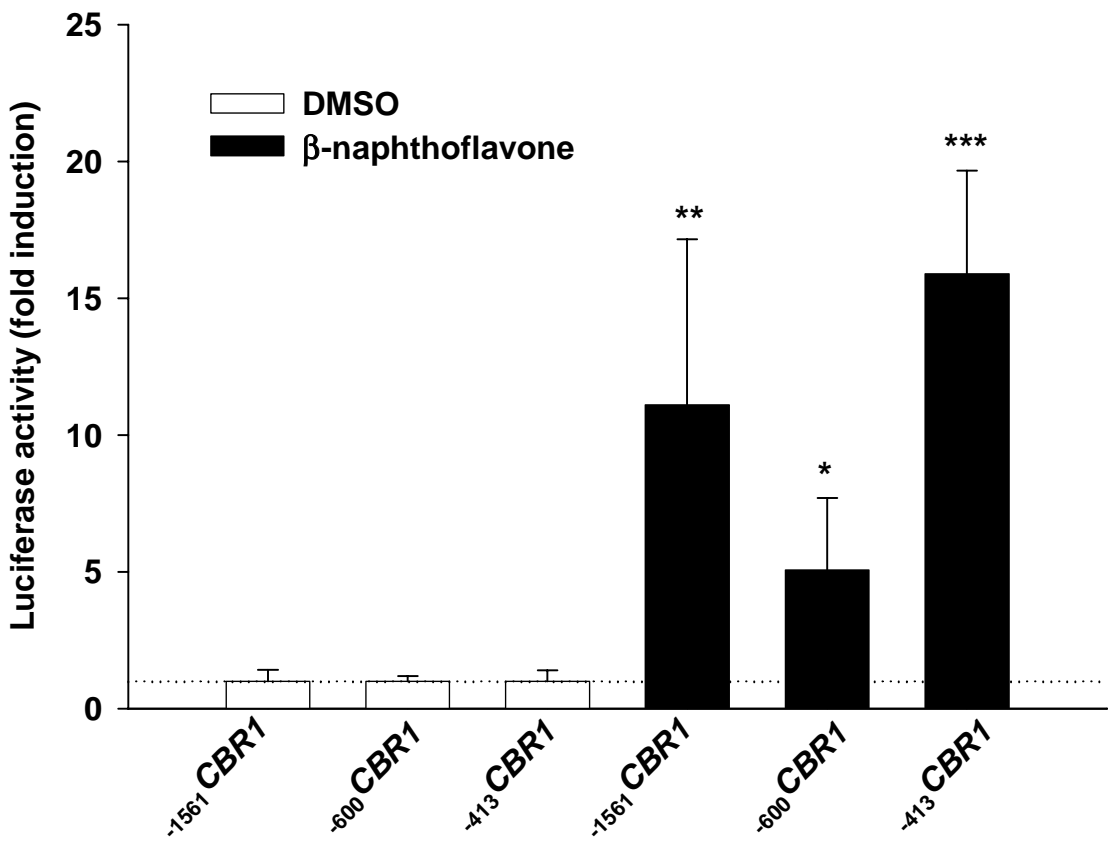


Figure 4

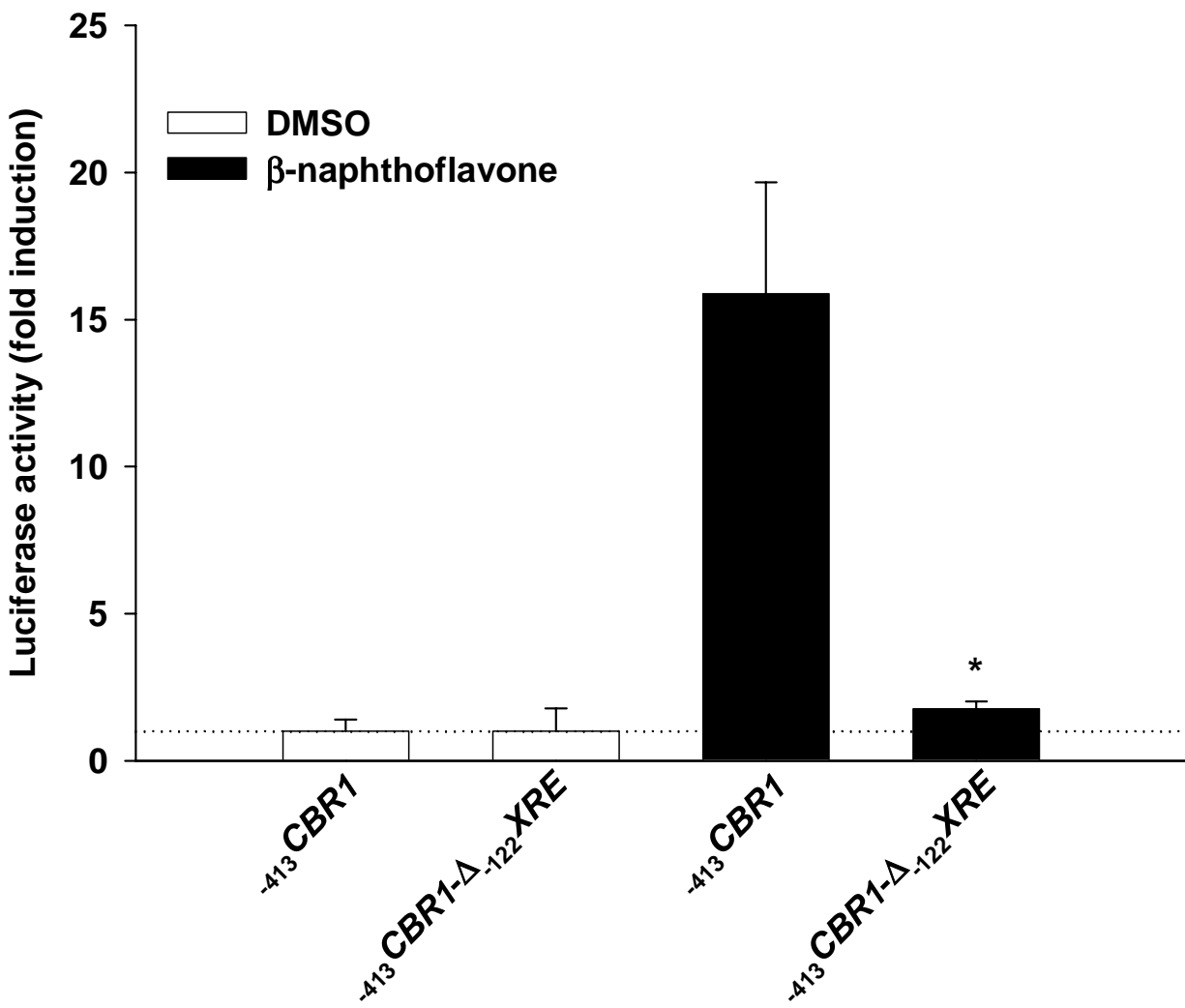


Figure 5

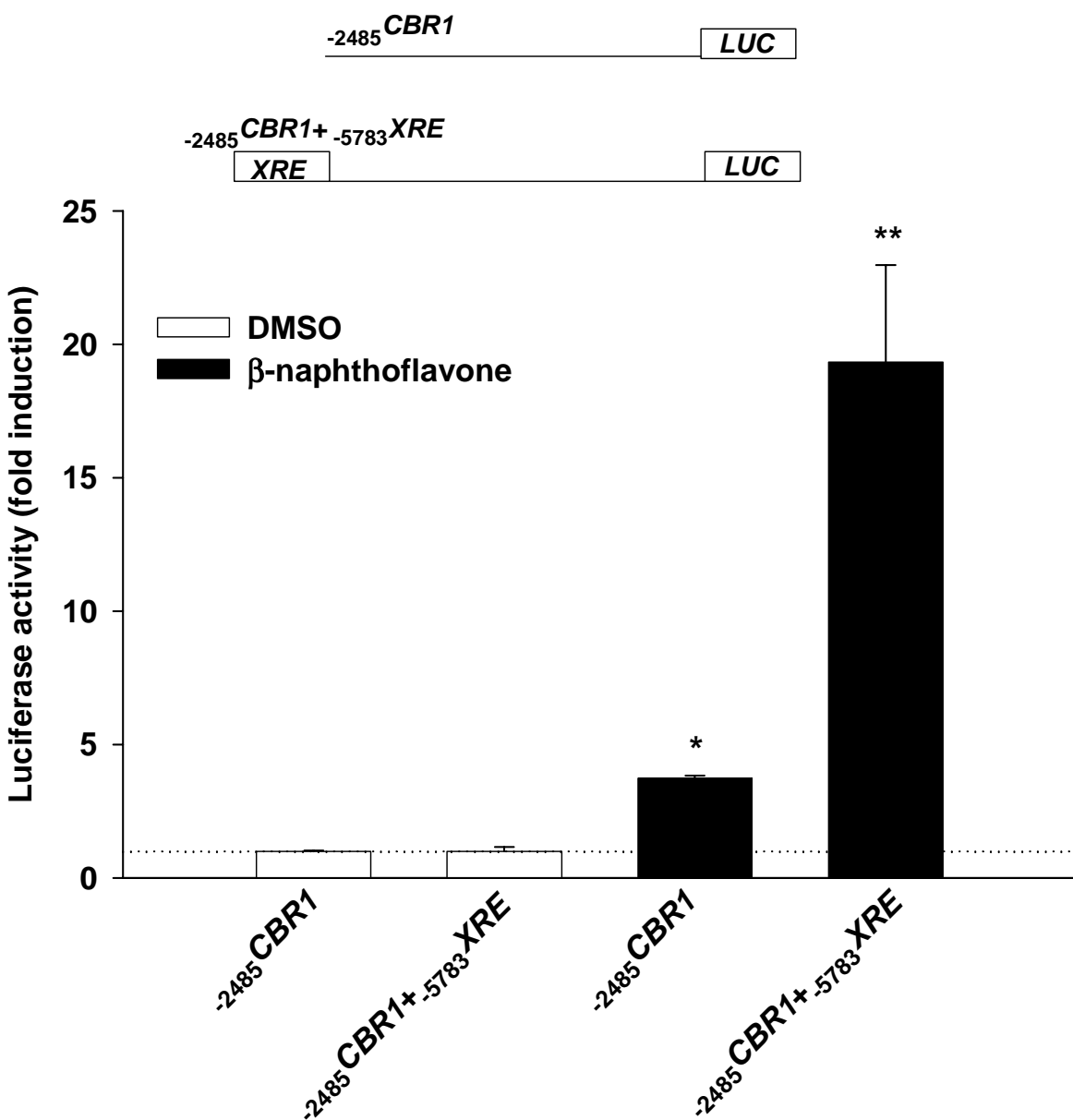


Figure 6

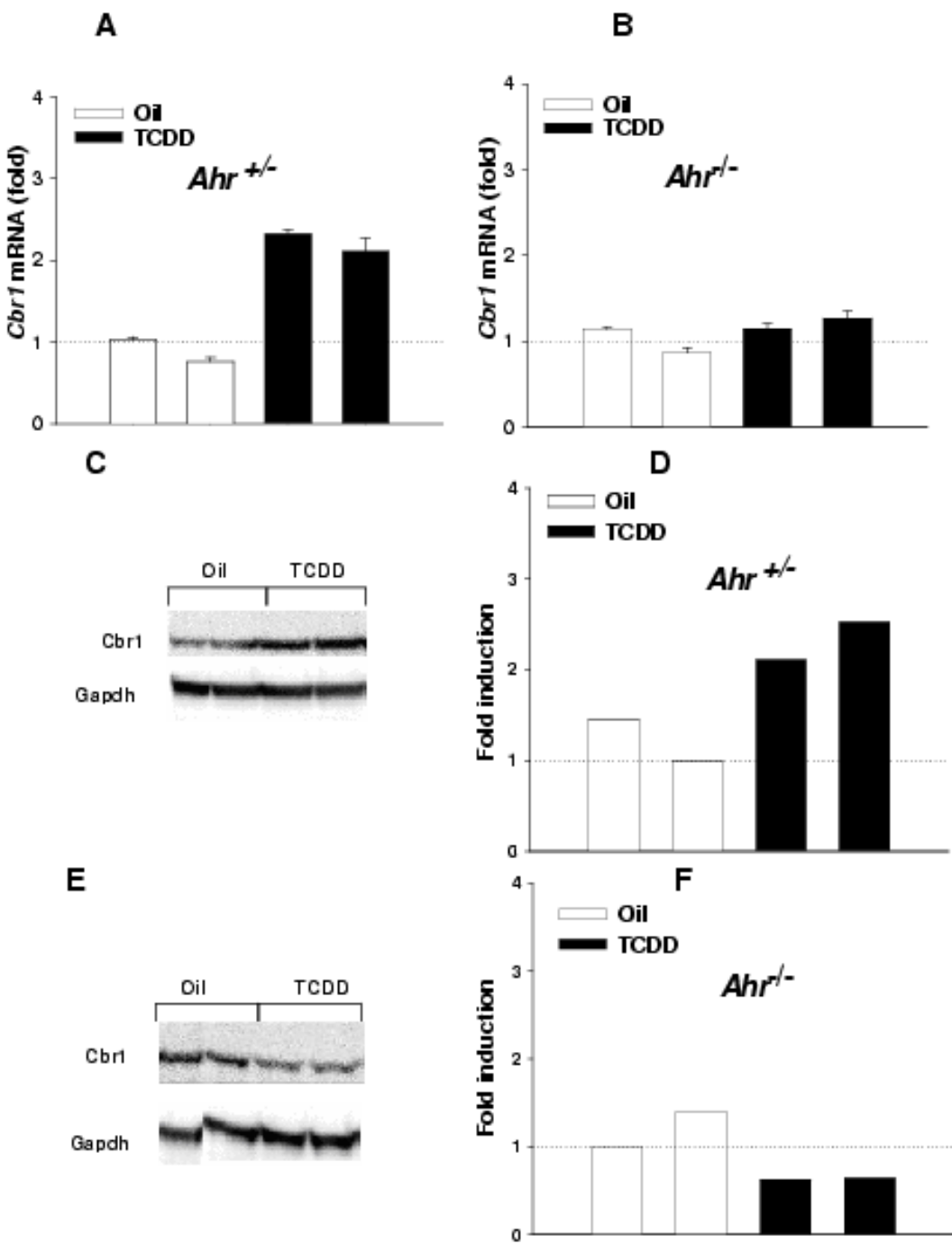


Figure 7

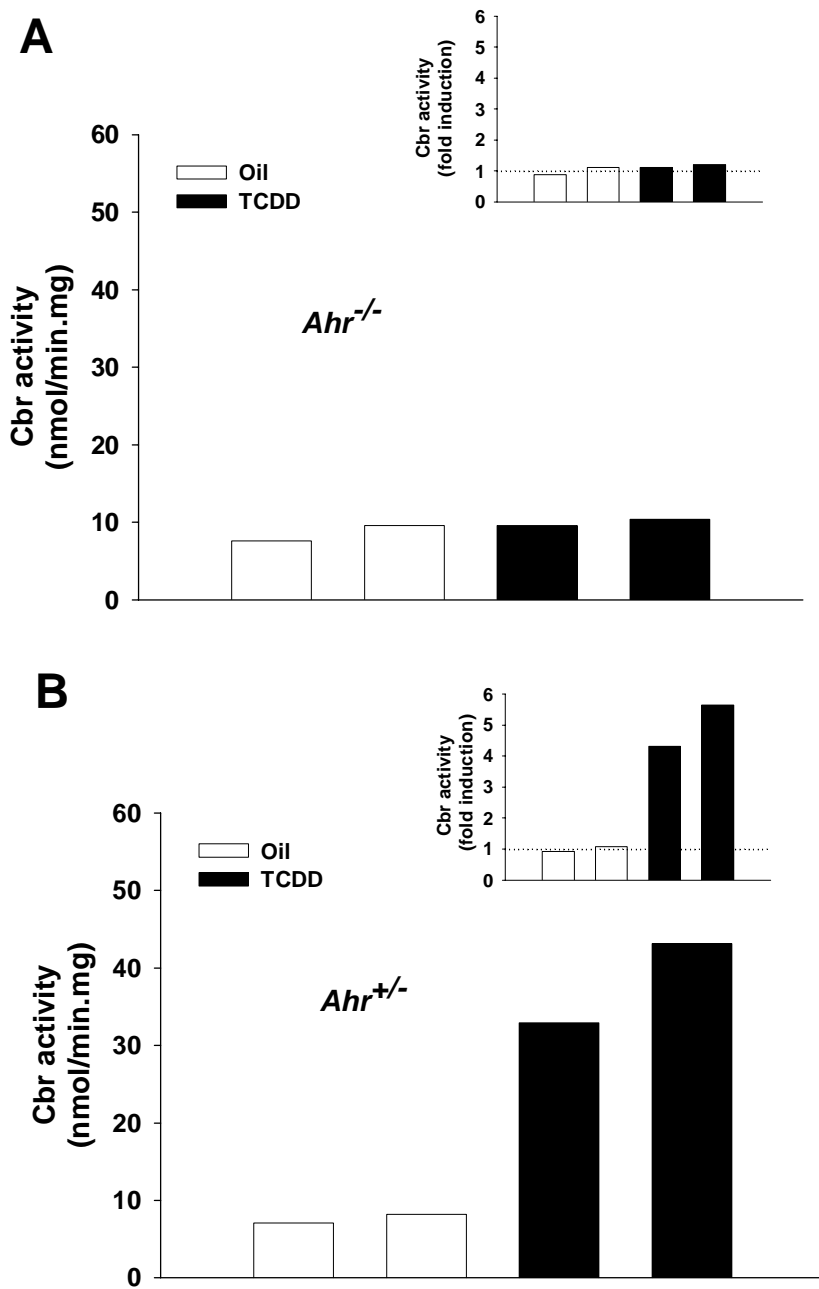


Figure 8

HUMANCBR1	GCAGTATTTTTTTAGATAACACCAGGAAAAAAAGAAAAAAAACCAT	-450
MOUSECbr1	TCTCTCTCTCTCGCCCTCCTGCAGTCAGTGCCTGGCAGCTGGCTT	
HUMANCBR1	GCAAATGTACTATTCTCAAACACAACAGGAATGATTGAAACAGCTGGG	-400
MOUSECbr1	CAA CACGC CTTCAGGAAAAGCCTGAGATGTCAGTCATTGACCTGGCCG	
	XRE	
HUMANCBR1	AGAATATGAAGAAAACCCCTCAGAGAACCAAGGGCAAGCAGTGAGTCAG	-350
MOUSECbr1	GTTCCTGGCTGGTATGTAACCCCCACTGCATAATGCATAATCTG	
HUMANCBR1	ATCTAGGCACATGCCACTAGGAATGGTTCTCACTGCCACGTGGCAGC	-300
MOUSECbr1	AGATAACAGACAACCTGACACCTTCGTTGCATGGTAAACTTTATTTAA	
HUMANCBR1	CAACAGCCAGTAGCTAGAGACCAGCCTCGGTCTCGGCCTGCAGGTTCTG	-250
MOUSECbr1	AAAAAAAACAAAAACAAAAAAACGGAGTTCAGGTAAAGGTGAGC	
HUMANCBR1	CAAAGTCAGGCTAGCTGGCTCTCCGCTGCTCCGCACCCGGGAGGGTTC	-200
MOUSECbr1	CATTTCTAAATACACAGCAATTGACAAGAGGCAACTTAAATCCACA	
	GC-BOX	SP1/GC-BOX
HUMANCBR1	CGGTGGGAGGGTAGGGATGGTTCA GCCCCGCCCC GCT AGGGCGGGGC C	-150
MOUSECbr1	CTAAACAACAAACACACCCCCCACCAGCCACGCCCGTAGGGAG GGGG	
	XRE	GC-BOX
HUMANCBR1	TGCGCCTGCGCGCTCAGCGGCCGG GCGTG TAACCCACGGGTGCGGCCCA	-100
MOUSECbr1	C TTAAACTGCGCAT GCGTG CTAGGTGCGACATTGTCGACGCCATTTCAG	
	XRE	
HUMANCBR1	CGACCGCAGACTCGAGCAGTCTCTGGAACACCGCTGCAGGGCTCCGGG	-50
MOUSECbr1	TCCGCCAGTGAACCGGTCTTGAACCACTCTCCAGCAGCCTCGAGAGGGCAG	
HUMANCBR1	CTGAGCCAGGTCTGTTCTCACGCAGGTGTTCCCGCGCCCCGTTAGCC	-1
MOUSECbr1	AGTTTGCGCCAAGTTCTTGGTCTCCGACGGCCTCCCTCTCACGCAGCC	

Figure 9